

Chapter 6

Ellipsometric study of porous silicon layers

The ellipsometric study of porous silicon monolayers and multilayers is presented in this chapter. The objective of this study is to determine the main physical characteristics of these layers: porosity (and therefore refractive index) and thickness. These characteristics have been previously calculated with other methods and the comparison between those results and the results obtained with ellipsometry is also presented. In addition, spectroscopic ellipsometry allows the analysis of the anisotropy of the porous layers. This characteristic can not be analyzed by any of the previous characterization methods used, so ellipsometry provides this additional data for the knowledge of the fabricated porous silicon layers.

First, in this chapter, we briefly explain the theoretical concepts of spectroscopic ellipsometry. Next, we describe the equipment used for the ellipsometric measurements, the ellipsometer. The different steps followed for the characterization of the porous silicon layers are also explained. After that, we show the most relevant results obtained from ellipsometry, firstly the

ellipsometric study of fabricated porous silicon monolayers, and secondly the study of porous silicon multilayers consisting of a periodic repetition of two layers with different degrees of porosity. Finally, we present the conclusions obtained from our experiments.

6.1. Introduction to Spectroscopic Ellipsometry

Ellipsometry is an optical characterization technique based on the measurement of the polarization transformation that occurs after the reflection (or the transmission) of a polarized beam by a given sample [209]. Ellipsometry is a well known technique that has been currently practiced since the second half of nineteenth century and it is supported by a complete theoretical description [209].

When a beam of linearly polarized light of a known orientation is reflected at oblique incidence from a surface then the reflected light is elliptically polarized, for this reason the term ellipsometer was chosen. The shape and orientation of the ellipse depend on the angle of incidence, the direction of the polarization of the incident light, and the reflection properties of the surface.

Nowadays ellipsometry has many interesting applications. In particular, it is mainly used in semiconductor research and fabrication to measure the optical properties as well as the physical dimensions of complex systems such as multilayer stacks of thin films and the interfaces between those layers [210-214]. However, ellipsometry is also becoming more interesting to researchers in other disciplines such as biology and medicine [215,216]. These areas pose new challenges to the technique, such as measurements on unstable liquid surfaces and microscopic imaging [217-219].

Ellipsometry is sensitive to several material characteristics, such as layer thickness, optical constants (refractive index and extinction coefficient), surface roughness, composition, optical anisotropy; and is used to characterize both single layers and multilayer stacks [218,220,221].

6.1.1. Fundamentals of ellipsometry

All the expressions that will be mentioned from now on will be related to reflection ellipsometry. Anyway, broad information can be found in the literature [222,223] about the instrumentation and the mathematical formalism of transmission ellipsometry.

In both reflection and transmission ellipsometry, the direction of the incident and reflected beams determine the plane of incidence. To easily introduce the basic ellipsometric magnitudes and to generalize them, we will first consider the case of a plane wave whose electric field vector can be decomposed into two components, one parallel (subscript p) and another perpendicular (subscript s) to the incidence plane. Fig. 6.1 shows the schematic representation of the incident \vec{E}^i and reflected \vec{E}^r fields, and their corresponding components E_p^i , E_s^i , E_p^r , and E_s^r .

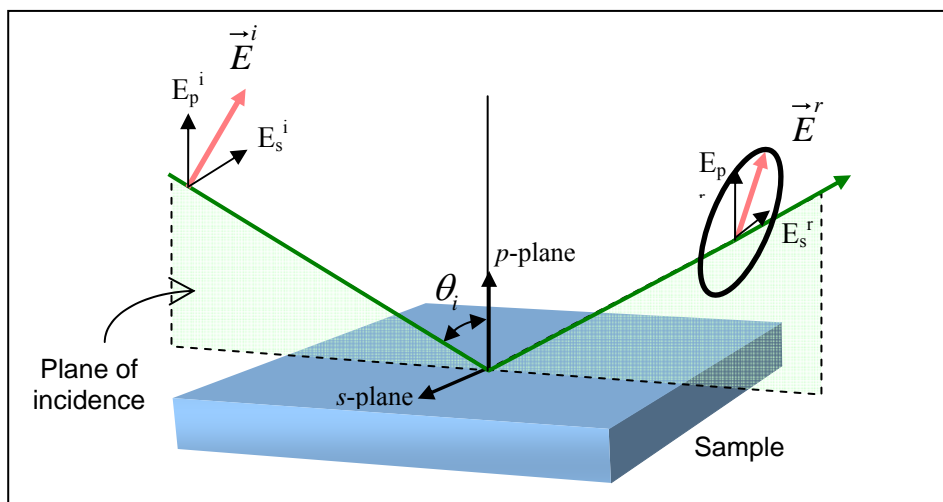


Fig. 6.1. Schematic of the incident electric field (\vec{E}^i) and the reflected electric field (\vec{E}^r).

These components are usually expressed in complex notation:

$$\vec{E}^{i,r} = \begin{pmatrix} E_p^{i,r} \\ E_s^{i,r} \end{pmatrix} = e^{j(\omega t - \vec{k}_0 \vec{z})} \begin{pmatrix} A_p^{i,r} \\ A_s^{i,r} \end{pmatrix} = e^{j(\omega t - \vec{k}_0 \vec{z})} \begin{pmatrix} \alpha_p^{i,r} e^{j\beta_p^{i,r}} \\ \alpha_s^{i,r} e^{j\beta_s^{i,r}} \end{pmatrix} \quad (6.1)$$

where ω is the angular frequency, \vec{k}_0 is the wavenumber vector in the vacuum, $A_p^{i,r}$ and $A_s^{i,r}$ are the complex amplitudes of the field components, $\alpha_p^{i,r}$ and $\alpha_s^{i,r}$ are their modulus and $\beta_p^{i,r}$ and $\beta_s^{i,r}$ are their relative phases for $t=0$ and $z=0$. As the physical magnitude actually detected by ellipsometers is the radiation intensity, the general phase, $e^{j(\omega t - \vec{k}_0 \vec{z})}$, is not considered because it does not affect the magnitude value. On the contrary, the relative phases are very important for the intensity value determination.

The p and s components of the incident and reflected electric fields are related to each other with the reflection coefficient in parallel polarization r_p and the reflection coefficient in perpendicular polarization r_s , respectively. The expressions of these two relations are:

$$\begin{aligned} A_p^r &= r_p A_p^i \\ A_s^r &= r_s A_s^i \end{aligned} \quad (6.2)$$

Ellipsometry measures the modulus and phase of the quotient between the reflection factor in parallel polarization and the reflection factor in perpendicular polarization. This quotient is named complex relation, ρ , and is expressed as:

$$\rho = \frac{r_p}{r_s} \quad (6.3)$$

From this relation the ellipsometric angles Ψ and Δ are defined as:

$$\rho = \tan \Psi e^{j\Delta} \quad (6.4)$$

where Ψ is the angle whose tangent is the quotient of the modulus of the reflection factors r_p and r_s and Δ is the phase change difference that the p and the s components undergo in the reflection.

Although the most used ellipsometric parameters are Ψ and Δ , for the study of the porous silicon layers we will study I_s and I_c , because these are the magnitudes actually measured in the setup we have used [224] The relation of these values with Ψ and Δ are

$$\begin{aligned}I_s &= \sin(2\Psi) \sin(\Delta) \\I_c &= \sin(2\Psi) \cos(\Delta)\end{aligned}\tag{6.5}$$

Because ellipsometry measures the ratio of two values, it can be highly accurate and very reproducible.

The most important application of ellipsometry is to study thin films. In the context of ellipsometry a thin film is one that ranges from essentially zero thickness to several thousand Angstroms, although this range can be extended in some cases. If a film is thin enough that it shows a colored interference pattern then it will probably be a good ellipsometric sample. The sensitivity of an ellipsometer is such that a change in film thickness of a few Angstroms is usually easy to detect.

The use of spectroscopic ellipsometry has many advantages. The most important one is that ellipsometry measures a ratio of two values which permits highly accurate and reproducible (even in low light levels) results. No reference sample is necessary and it is not as susceptible to scatter, lamp or purge fluctuations as other measurement techniques.

Ellipsometry provides two values at each wavelength so we obtain more information about sample and therefore more film properties. Some ellipsometers allow the variation of the incidence angle, being called Variable Angle Spectroscopic Ellipsometry (VASE) that report new information optimizing the sensitivity.

6.1.2. Equipments for ellipsometric measurements. Ellipsometers

There are many different ways of determining the polarisation of a beam of light. In the first ellipsometers, the operator observed the light beam that was reflected off the sample through an eyepiece. The polarisers and retarders were rotated by hand until the effect of the polarisation was inverted and no light would pass through the instrument. This is called the nulling technique. Many instruments are still based on the nulling technique although today's null ellipsometers are somewhat more sophisticated. The light sources used in these instruments were often fixed to a single wavelength.

Modern nulling ellipsometers use computers to rotate the elements and to automatically calculate the ellipsometry signal very quickly. However, the nulling technique is not ideal for automated instruments because it is based on measuring a zero signal. This was an advantage in the early ellipsometers because the human eye is very sensitive to small changes in the signal around the 'null'.

In recent years, the advent of computer control and multichannel detectors has made it possible to develop fast spectroscopic ellipsometers. A technique that is more suited to modern-day instrumentation is Phase Modulated Ellipsometry. The phase modulated ellipsometer (PME) is that in which the state of the radiation beam polarization in a certain point of its trajectory is modulated, obtaining information of the measured system with an analysis of the harmonics of the detected signal.

The most relevant advantages of the PME are the absence of mechanical vibrations of the optical elements and the high modulation frequency that allows the fast data acquisition, that makes possible the monitoring of processes of preparation and treatment of samples in real time.

6.2. Ellipsometric characterization process

The characterization of porous silicon layers using spectroscopic ellipsometry has been realized during my stage at the École polytechnique in Palaiseau (France), under the supervision of Dr. Enric García-Caurel. Part of the ellipsometric measurements were also realized at Horiba Jobin Yvon in Longjumeau (France). During this stage many porous silicon monolayers and multilayers were measured and characterized. In this section, the equipment and the process for the measurement and characterization of the layers are detailed.

6.2.1. UVISEL Ellipsometer

All the fabricated porous silicon layers have been measured using the UVISEL NIR Spectroscopic Phase Modulated Ellipsometer commercialized by HORIBA-Jobin Yvon. The ellipsometric data were acquired at an incident angle of 70° (some measurements for 55°) for the wavelength range 0.9-1.8 μm with a step of 10 nm.

Fig. 6.2a shows the photograph of the UVISEL ellipsometer used for the realization of the measurements. In Fig. 6.2b we can observe the different parts of this equipment [225].

Fig. 6.2b shows a schematic representation of the optical setup of the phase-modulated ellipsometer. The light source is a xenon lamp, which emits unpolarized light. The beam is focused on the entry of an optical fiber and then passes through a polarizer. After reflection on the sample, the beam is analyzed by a Photoelastic Modulator (PEM) with a 50 kHz modulation frequency, and a second polarizer called analyzer. The light intensity is then introduced to a spectrograph to process the data acquired.

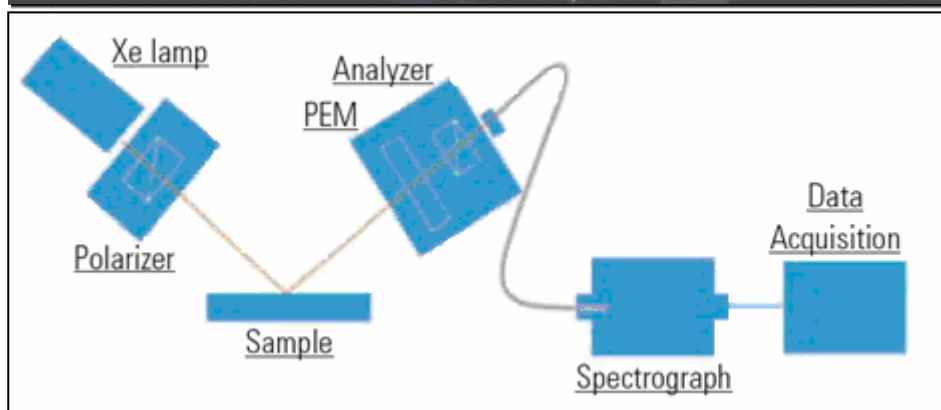


Fig. 6.2. a) UVISEL ellipsometer (École polytechnique) b) Schematic of the UVISEL ellipsometer elements [After 225].

6.2.2. Influence of the spot size on the ellipsometric measurements

Two different sets of samples have been characterized by ellipsometry. Each set has been fabricated using a different electrochemical cell: one set was fabricated with the lateral-wafer cell and the other with the bottom-wafer cell.

In section 5.1.1, we have concluded that the porous silicon layers obtained with the lateral wafer cell were very inhomogeneous, being the bottom-wafer cell the most appropriate for the fabrication of homogeneous porous silicon layers.

The inhomogeneity of the porous layers obtained with the lateral cell can be also observed from the ellipsometric measurements of the porous silicon layers. The spot size of the beam for the ellipsometric measurement can be adjusted in the UVISEL ellipsometer. Three different spot sizes can be selected: macrospot (1 x 2 mm), mesospot (0.1 mm x 0.2 mm) and microspot (0.01 mm x 0.02 mm). The ellipsometric measurement is an average of the measurement in the spot area. If the refractive index and/or the thickness across the spot area are different the resulting ellipsometric measurement will lead to an averaged result which cannot be fitted because averaging is not taken into account by our ellipsometry software. In consequence, it is very important to choose the appropriate spot size for each type of layer. For inhomogeneous layers the smallest spot size, the microspot is the most suitable whereas the homogeneous layers can be measured with a better signal-to-noise ratio with the meso or the macrospot.

Our porous silicon monolayers, obtained with both electrochemical cell types, have been measured with the three spot sizes. Fig. 6.3 shows the ellipsometric measurements realized to a porous silicon monolayer obtained with the lateral-wafer cell for two different spot sizes. We can observe that the results obtained are very different for the macrospot and for the mesospot. With the mesospot all the maxima and minima of I_S and I_C can be observed whereas with the macrospot these variations are attenuated and some of them are lost. This effect of aliasing is explained by the inhomogeneity of the samples, which corroborates the conclusions obtained in section 5.1.1 that the wafers obtained with the lateral-wafer cell are inhomogeneous.

Fig. 6.4 shows the ellipsometric measurements of a monolayer fabricated with the bottom-wafer cell. We can observe that I_S and I_C do not vary with the spot size, which indicates that the porous silicon monolayer is very homogeneous. The little variations of I_C at the maxima of the mesospot

measurements are not relevant, they are produced by the low signal-to-noise ratio of the instrument due to the small size of the spot.

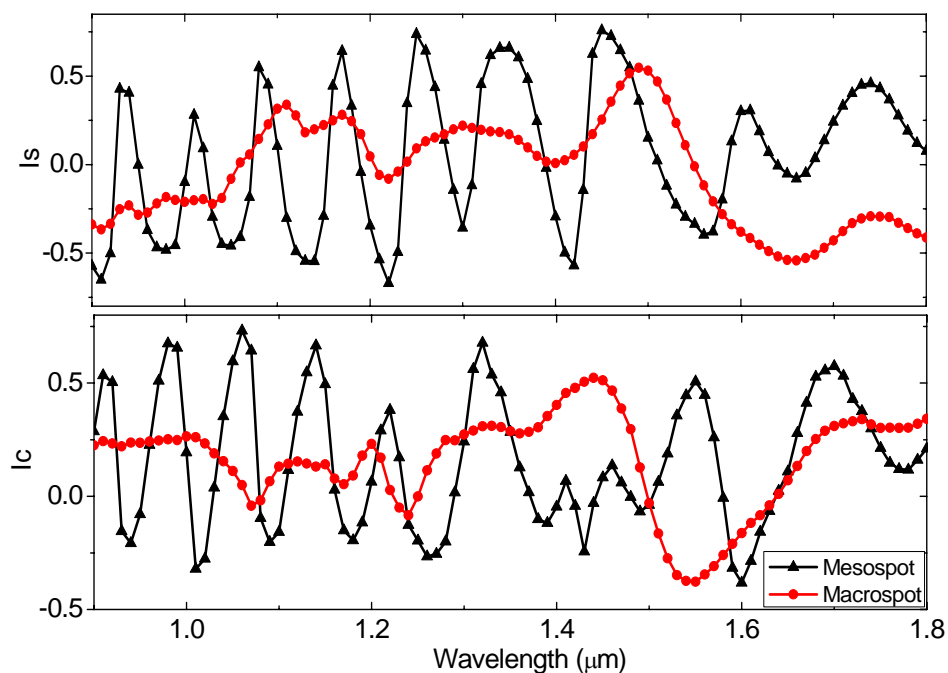


Fig. 6.3. Ellipsometric measurements of a porous silicon monolayer, fabricated with the lateral-wafer cell, for two different spot sizes.

The ellipsometric study has been realized for layers fabricated with both lateral and bottom-wafer cells. The results obtained with the latter cell are more accurate due to the homogeneity of the fabricated porous silicon layers. For this reason, in the next sections we only present the ellipsometric study realized for the bottom-wafer cell layers and the conclusions obtained from this study. The same conclusions have also been obtained for the lateral-wafer cell layers although the possible errors introduced in the characterization are slightly higher due to inhomogeneity.

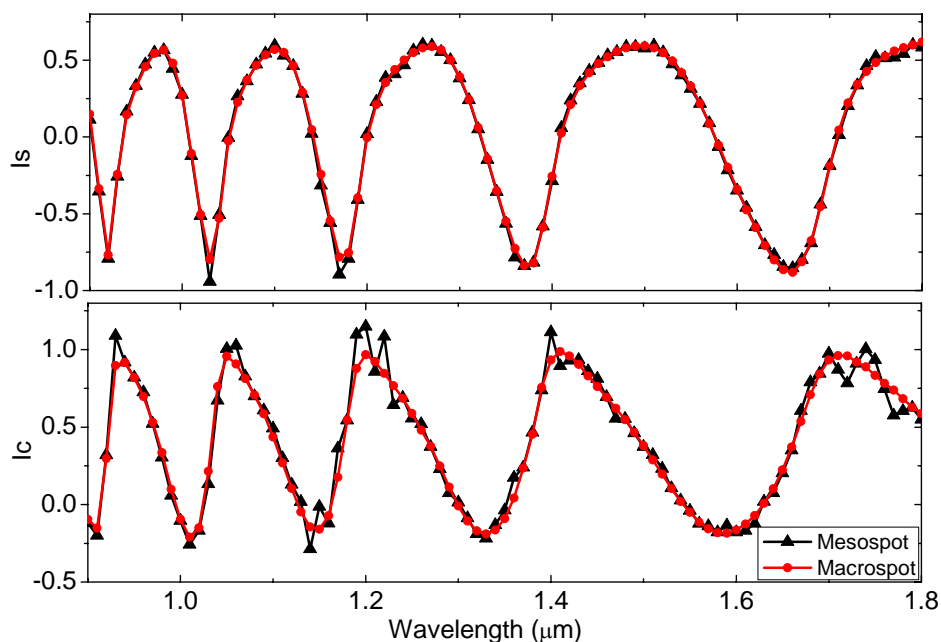


Fig. 6.4. Ellipsometric measurements of a porous silicon monolayer, fabricated with the bottom-wafer cell, for two different spot sizes.

6.2.3. Process for the determination of porous silicon characteristics using ellipsometric data

The characterization of porous silicon layers using spectroscopic ellipsometry is realized in two very different steps. Firstly, we measure the samples with the ellipsometer to obtain the experimental ellipsometric data, and second, we modelize the experimental data to interpret the measurement in terms of a physical model that connects the optical response with the physical structure of the given sample.

The optical model has been built using the DeltaPsi2 program, developed and commercialized by Jobin Yvon. A porous silicon layer has been modeled as a layer formed by two different materials, silicon and air (void), on a silicon crystalline substrate [226,227]. The law of mixture used to model the equivalent

dielectric function of the materials is the effective medium approximation of Bruggeman [228].

Although we have considered that a porous silicon layer is only formed by silicon and air, the existence of silicon dioxide could also be assumed. However, silicon dioxide has not been used for the model because its optical response is very similar to that of air and it is not possible to distinguish between their contributions.

Unknown parameters of this optical model can be thin film thickness, or optical constants or both. For our particular case, the unknown parameters are the thickness, and the volume fraction of void (porosity). The possible presence of uniaxial birefringence in the layers is also considered.

Using this optical model we have generated the simulated ellipsometric data. The unknown parameters are varied to try and produce the best fit between the simulated and the experimental ellipsometric data.

Numerical algorithms are used to vary the unknown parameters and minimize the difference between simulated and experimental data. In our particular case, we have used the Marquardt [229] minimization routine for the determination of porous silicon layers parameters. According to the article of Jellison [230] we have used a non biased mean-squared error (χ^2) function to measure the goodness of fit. The χ^2 is defined as follows

$$\chi = \frac{1}{2M-1} \sqrt{\sum_i \left[\frac{(I_{S_{T_i}} - I_{S_{X_i}})^2}{\sigma_{is}^2} + \frac{(I_{C_{T_i}} - I_{C_{X_i}})^2}{\sigma_{ic}^2} \right]} \quad (6.6)$$

where M is the number of points, $I_{S_{T_i}}$ is the simulated value Is for the i point, $I_{S_{X_i}}$ is the experimental value Is for the i point, $I_{C_{T_i}}$ is the simulated value Ic for the i point, $I_{C_{X_i}}$ is the experimental value Ic for the i point and σ_{is} and σ_{ic} are the error in the experimental determination, for this case $\sigma_{is} = \sigma_{ic} = 0.01$.

6.3. Measurement and characterization of porous silicon monolayers

Several porous silicon monolayers have been fabricated with the fabrication method explained in detail in chapter 5. Each of them has been obtained applying a different current density, therefore each monolayer has a different porosity, and so a different refractive index. Although a set of monolayers has been fabricated with each of the two types of anodization cell, in this and the next sections we only present the ellipsometric study realized for the bottom-wafer cell layers for the reasons explained in the previous section.

Each monolayer is identified by the current density (J) applied during the fabrication process because it determines its porosity (refractive index). For each porous silicon monolayer we have measured the ellipsometric data, determined the optical model with the best fit parameters (thickness and porosity), and evaluated the difference between the measured and the simulated ellipsometric data. The isotropy/anisotropy of the porous layers has also been analyzed.

All the ellipsometric characterization procedure is presented in this section. For clarity reasons, the monolayers have been grouped according to the optical model used for their characterization. We have found that depending on the value of the current density, the porous silicon layers show either an isotropic or an anisotropic optical response.

Besides, the thicknesses and the refractive indices determined with the ellipsometric data have been compared with the ones obtained by SEM and by the measurement of the interference fringes method (MIF method), respectively.

6.3.1. Isotropic optical model

The lowest current density used for the fabrication of our porous silicon monolayers is $J=10$ mA/cm². For his reason, this is the monolayer with the lowest porosity, and therefore with the highest refractive index. The monolayer has been obtained applying $J=10$ mA/cm² for 120 s. Fig. 6.5 shows the cross

section SEM image of this monolayer. The thickness estimated from the SEM image is approximately $1.32 \mu\text{m}$.

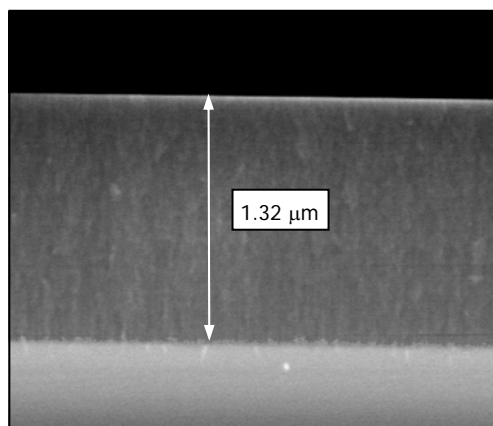


Fig. 6.5. Cross section SEM image of the porous silicon monolayer obtained with $J=10 \text{ mA/cm}^2$ and anodization time 120 s. The thickness is $1.32 \mu\text{m}$.

For the analysis of the measured ellipsometric data, the layer has been firstly assumed to be isotropic and composed of silicon and void (air). The optical model used for the characterization of this monolayer can be observed in Fig. 6.6a. It has been necessary to suppose that the monolayer is formed by two homogeneous and isotropic layers with different porosity because all the fits realized assuming only one isotropic layer had a too high χ^2 . The parameters that have been varied for obtaining the best fit are the thickness and the porosity of both layers. The best fit parameters obtained for this two isotropic layer model can also be observed in Fig. 6.6a whereas Fig. 6.6b shows both the measured and the simulated ellipsometric data obtained with this model, with $\chi^2=36.4$.

From Fig. 6.6a we can observe that the total thickness of the porous layers is 1.27 μm , very similar to the thickness estimated with SEM. The porosity of the top layer is higher than the one of the bottom layer, which is in line with the fabrication process, as the top layer is longer in contact with the electrolyte.

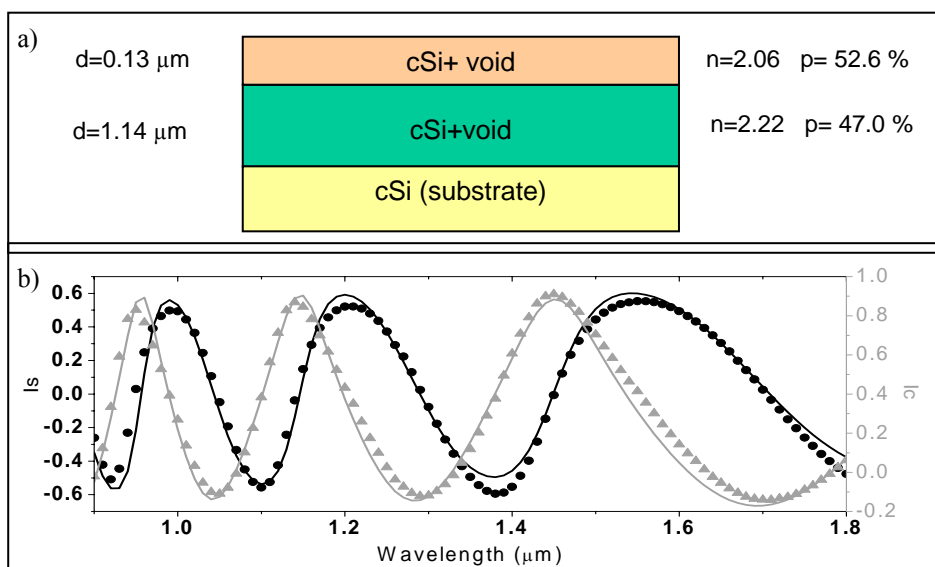


Fig. 6.6. a) Optical model consisting of two isotropic layers, the best fitted parameters (thickness, porosity) and refractive index for $\lambda=1.8 \mu\text{m}$ b) Measured ellipsometric data (dots) and simulated ellipsometric data obtained with the optical model (line).

The porosity, that is the volume fraction of air in the silicon layer, determines the refractive index. This refractive index is not constant within the wavelength range measured by the ellipsometer (from 0.9 to 1.8 μm) it decreases as the wavelength increases. The variation of the refractive index within this wavelength range depends on the porosity level but it is lower than 3%.

We compare now the refractive index obtained with ellipsometry with the one obtained with the MIF method. According to the details given in section 5.2.2.1, we recall that the MIF method gives a refractive index within the wavelength range instead of a punctual value for each wavelength. To ease the comparison of the refractive indices obtained with both methods, we will compare the one obtained with ellipsometry for $\lambda=1.8 \mu\text{m}$ with the highest refractive index obtained with the MIF method, because $\lambda=1.8 \mu\text{m}$ is the closest wavelength to the wavelength range analyzed with the MIF method. For this reason, all the refractive indices calculated with the MIF method that will be presented in this and the next sections will be approximate values.

The refractive index obtained with the MIF method for this monolayer is $n \approx 2.05$. The refractive indices obtained from ellipsometry are $n_t=2.06$ the top layer and $n_b=2.22$ for the bottom layer, at $\lambda=1.8 \mu\text{m}$. We can observe that although the refractive index of the top layer is very close to the one obtained with the MIF method, for the bottom layer the refractive index is more different.

Several studies concerning the fabrication process of porous silicon indicate that the porosity of a layer varies with depth [19,231], being the porosity at the top of the layer higher than the one at the bottom. It is known that once a porous silicon layer is formed no more electrochemical etching occurs but a slow chemical one starts, due to the permanence in HF [232,233]. This explains the fact that the top porosity is higher than the bottom porosity and it also leads to think that the variation of this porosity could be gradual in depth. From the analysis of ellipsometric measurements with the isotropic optical model we have already stated that this porosity variation exists in our layers. Now we are going to study whether a graded layer optical model can improve the description of the variation of porosity with thickness and consequently, the quality of fits of ellipsometric data.

Our optical simulation software represents a single graded layer as a multilayer stack made of a given number of homogeneous slices where the porosity changes slightly from slice to slice. Fig. 6.7a shows the graded optical

model, where the porosity decreases from top to bottom in a graded way. The parameters determined for the best fit are also shown.

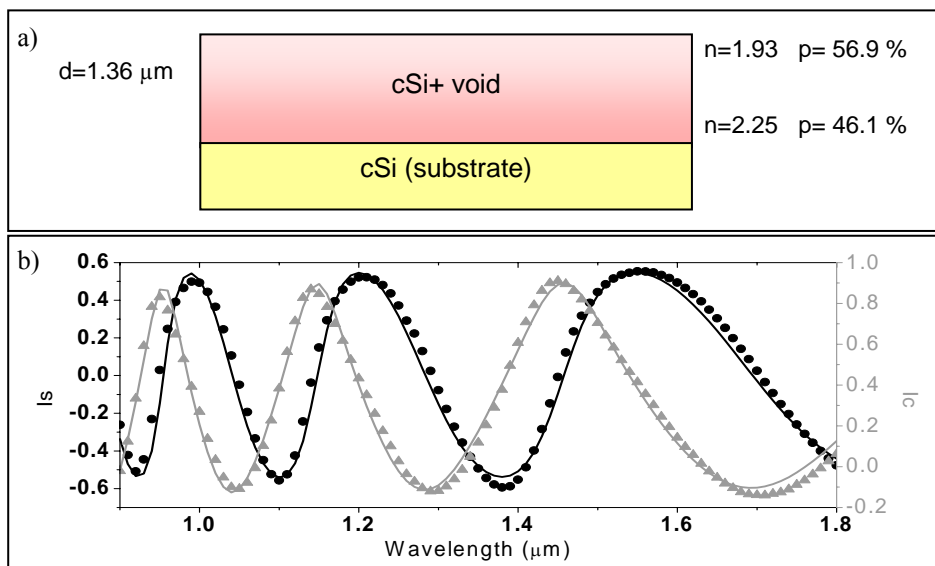


Fig. 6.7. a) Optical model with one gradient layer, the best fit parameters (thickness, and porosity) and refractive index for $\lambda=1.8 \mu\text{m}$ at the top and bottom of the graded layer. b) Measured ellipsometric data (dots) and simulated ellipsometric data obtained with the optical model (line).

We can observe that the thickness of this monolayer is closer to the thickness estimated with SEM ($1.32 \mu\text{m}$). The difference between these two thicknesses is very low and we can consider it as negligible because it could be introduced by the low accuracy of the SEM image.

The refractive indices obtained with this model are $n_t=1.93$ at the top of the layer and it gradually increases towards the bottom until a value of $n_b=2.25$, both for $\lambda=1.8 \mu\text{m}$. To better compare these values with the one obtained with the MIF method we have calculated the average refractive index of the monolayer with $n_{\text{average}}=(n_t+n_b)/2$. The average refractive index is $n_{\text{average}}=2.09$

and n with the MIF method is 2.05. We can observe that they are almost equal. The small difference can be attributed to the dispersion of the refractive index with the wavelength.

The comparison between the measured and the simulated ellipsometric data can be observed in Fig. 6.7b. The value of χ^2 for the gradient model is lower (25.9) than the value of the same function corresponding to the homogeneous model (36.4).

From these results we conclude that the fit realized with the gradient optical model is better than the one realized with the homogeneous model for the following reasons: the thickness obtained is closer to the thickness estimated with SEM, the value of χ^2 is lower which means that variation of porosity with depth is better simulated, the average refractive index of the optical model is very close to the calculated with MIF method.

Therefore, we can conclude that this is an isotropic layer where the porosity decreases gradually from top to bottom.

The same graded isotropic optical model has been used for the characterization of a porous silicon monolayer obtained with $J=14$ mA/cm². This current density is higher than the one of the previous monolayer, so the porous silicon monolayer obtained is expected to have a higher porosity, and therefore a lower refractive index. The anodization time for the formation of this monolayer was $t=90$ s. The thickness of this layer is approximately 1.35 μm (SEM image) and the refractive index calculated with the MIF method is approximately $n \approx 1.97$.

The optical model for this monolayer can be observed in Fig. 6.8a. The best fit is obtained for thickness 1.3 μm and porosity varying gradually from 60.3 % at the top to 48.8 % at the bottom. For this porosity, the refractive indices are $n_t=1.83$ and $n_b=2.17$, being the averaged value $n_{\text{average}}=1.99$ ($\lambda=1.8$ μm). It can be observed that both the refractive index and the thickness obtained with the ellipsometric characterization agree with the values obtained with the MIF method and SEM, respectively. The ellipsometric data simulated with the

optical model can be compared with the measured data in Fig. 6.8b, where χ^2 is 81.4.

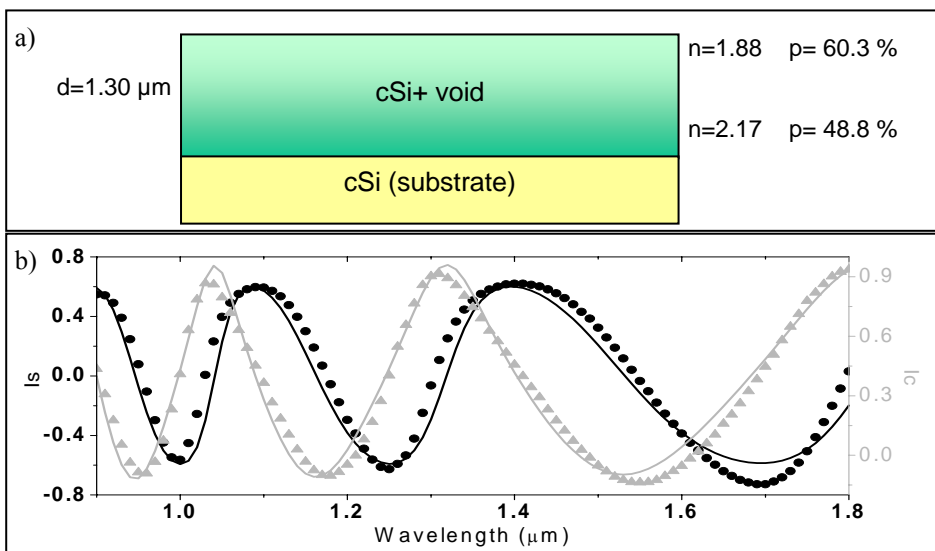


Fig. 6.8. a) Optical model with one gradient layer, the best fit parameters (thickness, and porosity) and refractive index for $\lambda=1.8 \mu\text{m}$ at the top and bottom of the graded layer. b) Measured ellipsometric data (dots) and simulated ellipsometric data obtained with the optical model (line).

6.3.2. Anisotropic optical model

The porous silicon layers presented in this section have been obtained with current densities higher than 14 mA/cm^2 , therefore their porosity is higher than the one of the previous monolayers.

The first monolayer to be characterized is the one obtained with $J=20 \text{ mA/cm}^2$. The refractive index calculated with the MIF method is 1.92 and the thickness from the SEM image (see Fig. 6.9) is $2.48 \mu\text{m}$.

The ellipsometric data from this porous silicon monolayer has been also modeled with a graded isotropic layer as the previous monolayers. This optical model can be observed in Fig. 6.10a together with the best-fitted values of the thickness and the porosity. The average refractive index for $\lambda=1.8 \mu\text{m}$ is 1.98, that is similar to the MIF refractive index. However, the thickness obtained with ellipsometry is lower than the one estimated with SEM and the difference between the measured and the simulated ellipsometric data (Fig. 6.10b) is very high, $\chi^2=286.8$.

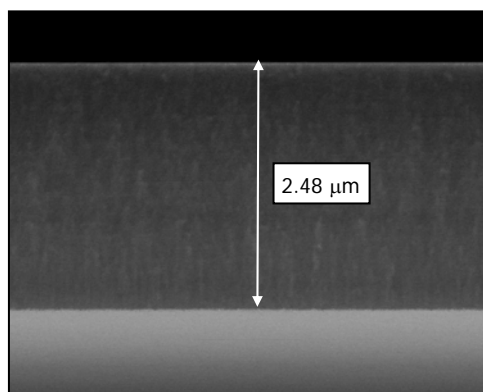


Fig. 6.9. SEM image of the porous silicon monolayer obtained with $J=20 \text{ mA/cm}^2$ and anodization time 120 s. The thickness is $2.48 \mu\text{m}$.

From these results, we can deduce that an isotropic graded layer is not the most appropriate optical model for the simulation of this porous silicon monolayer. The only difference between this monolayer and the previous ones is the higher current density used for its formation, that leads to higher porosity. Hence, we can deduce that the isotropic graded layer model is appropriate only for low porosity porous silicon layers ($J \leq 14 \text{ mA/cm}^2$).

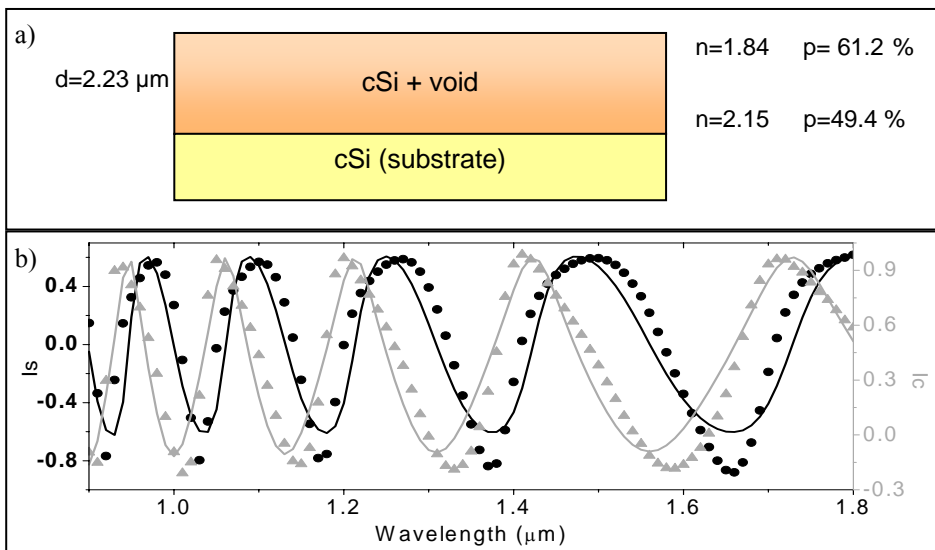


Fig. 6.10. a) Optical model with one gradient layer, the best fit parameters (thickness, and porosity) and refractive index for $\lambda=1.8 \mu\text{m}$ at the top and bottom of the graded layer. b) Measured ellipsometric data (dots) and simulated ellipsometric data obtained with the optical model (line).

Another optical model has been studied consisting of an anisotropic layer [231,233,234]. The difference between an isotropic and an anisotropic material can be schematically observed in Fig. 6.11. An isotropic material is the one that has the same optical properties in all directions [204]. In the case of the refractive index, it means that the refractive index is the same in all directions. Anisotropy is the property of being directionally dependent, that is, the material has different physical properties (in this case refractive index) along different axes [204]. For the simulation of this porous silicon layer, we have supposed that the material is uniaxial and birefringence can be formalized by assigning two different refractive indices to the material for different polarizations. The birefringence magnitude is then defined by:

$$\Delta n = n_e - n_o \quad (1)$$

where n_o and n_e are the refractive indices for polarizations perpendicular (ordinary) and parallel (extraordinary) to the axis of anisotropy respectively.

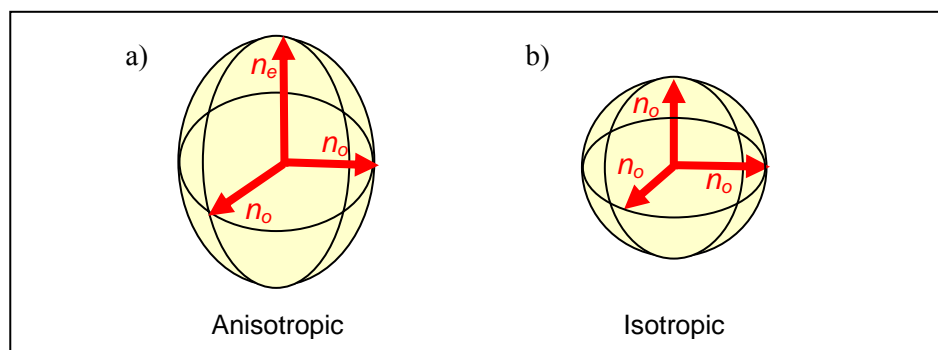


Fig. 6.11. Refractive index for every direction in an isotropic material (a) and anisotropic material (b).

The anisotropic optical model for the simulation of this porous silicon layer can be observed in Fig. 6.12a. The axis of anisotropy is perpendicular to the layer surface. The best fit with this model is obtained for thickness $2.44 \mu\text{m}$ and for refractive index $n_e=2.01$ and $n_o=1.82$ at $\lambda=1.8 \mu\text{m}$, being the averaged value $n_{\text{average}}=1.91$. Although the MIF method does not consider the anisotropy of the layer, we can compare the refractive index obtained with MIF (1.92) with the average value of the optical model. We can observe that the refractive indices and the thicknesses obtained with both methods agree. In Fig. 6.12b we can compare the simulated and the measured ellipsometric data, being $\chi^2=46.4$, which is remarkably lower than the value obtained with the graded model.

This good agreement and the low value of χ^2 obtained with the anisotropic model, lead us to conclude that when the porosity of the porous silicon layer increases, the material is not isotropic but it has an anisotropic behavior.

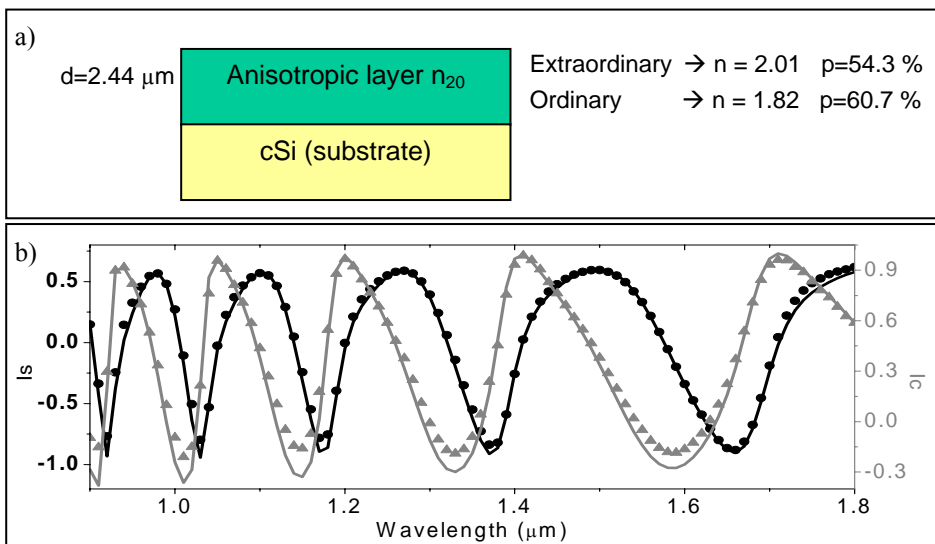


Fig. 6.12. a) Optical model consisting of an anisotropic layer, its best fit parameters (thickness, porosity) and the refractive index ($\lambda=1.8 \mu\text{m}$) for the extraordinary and the ordinary axes b) Measured ellipsometric data (dots) and simulated ellipsometric data obtained with the optical model (line).

Notice that the extraordinary refractive index is higher than the ordinary refractive index. This indicates that in one direction the quantity of air is higher than in the other direction. This agrees with the fabrication process because it is known that the anodization preferentially occurs at the pore tips and that the etching of the porous silicon proceeds in depth with an overall directionality which follows the anodic paths inside silicon.

From these results we could conclude that for $J \leq 14 \text{ mA/cm}^2$, the difference between the extraordinary and the ordinary refractive indices is small enough to be masked by the in depth inhomogeneity, whereas for $J > 14 \text{ mA/cm}^2$ the anisotropy is more important than the inhomogeneity.

The observed anisotropic behavior of the high porosity layers has also been studied with the ellipsometric characterization of two other high porosity layers: $J=30 \text{ mA/cm}^2$ and $J=50 \text{ mA/cm}^2$.

The monolayer obtained with the application of $J=30 \text{ mA/cm}^2$ for 120 s has $n \approx 1.73$ (MIF method) and thickness of approximately $3.28 \text{ }\mu\text{m}$ (SEM). The best fit with the anisotropic optical model is obtained for thickness $3.28 \text{ }\mu\text{m}$ (the same as the one estimated with SEM) and refractive indices $n_e=1.8$ and $n_o=1.64$ (Fig. 6.13), being $n_{\text{average}}=1.72$. The value of the merit figure χ^2 is 60.5, leading to the conclusion that this anisotropic optical model is appropriate for this porous silicon layer.

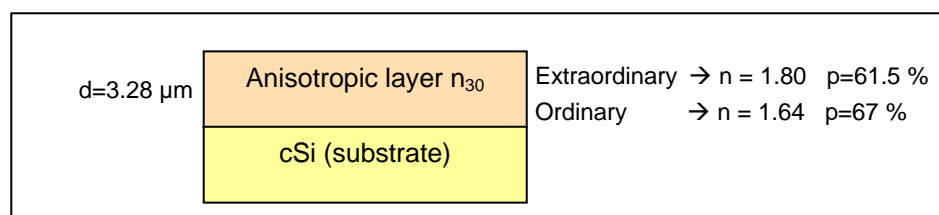


Fig. 6.13. Optical model consisting of an anisotropic layer, the best fit parameters (thickness, porosity) and the refractive index ($\lambda=1.8 \text{ }\mu\text{m}$) for the extraordinary and the ordinary axes.

Finally, let's consider the last porous silicon monolayer characterized with ellipsometry, that is the one obtained with $J=50 \text{ mA/cm}^2$ for 60 s. Its thickness is approximately $2.37 \text{ }\mu\text{m}$ (SEM) and the refractive index calculated with the MIF method is $n \approx 1.45$.

The anisotropic optical model used for this monolayer can be observed in Fig. 6.14a. The experimental and simulated ellipsometric data are shown in Fig. 6.14b, where we can observe that the agreement is good with a merit function $\chi^2=100.5$. For this layer, the most porous of the monolayers set, the fit of the simulated to the measured ellipsometric data has been the most difficult

of all and the χ^2 obtained with this model is slightly higher than for the rest of monolayers. In spite of this difficulty, the parameters obtained with ellipsometry are very close to the parameters obtained with by SEM and MIF: the thickness difference is only 90 nm (about 4 %), that could be due to the inaccuracy of the SEM estimation; and the average refractive index is $n_{\text{average}}=1.47$ very close to the MIF refractive index (1.45).

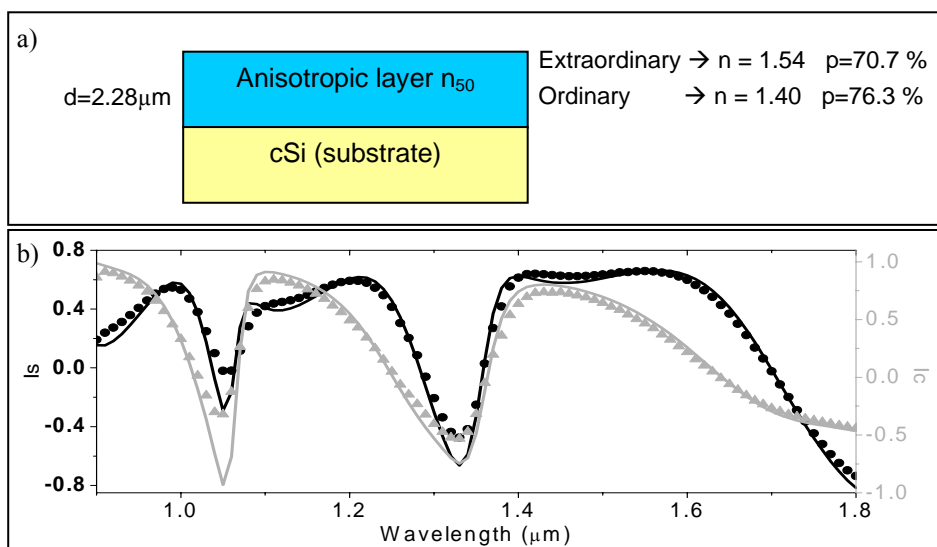


Fig. 6.14. a) Optical model consisting of an anisotropic layer and its best fit parameters: thickness, porosity and refractive index ($\lambda=1.8 \mu\text{m}$) for the extraordinary and the ordinary axes b) Measured ellipsometric data (dots) and simulated ellipsometric data obtained with the optical model (line).

Therefore, we can conclude that the anisotropic optical model is the most appropriate for high porosity layers.

6.3.3. Depolarization of porous silicon layers

From the ellipsometric study of these porous silicon monolayers we have observed that the difference between the measured and the simulated ellipsometric data, quantified with χ^2 , was different for each layer. Specifically, χ^2 increased when the current density, and hence the porosity, increased. This can be due to the fact that the anisotropy of porous silicon produces the depolarization of light. If the sample depolarizes the light, the ellipsometric angles (Δ and Ψ) are not well defined, because they were measured under the supposition that there is no depolarization.

To explain the increment of χ^2 with the current density, we have measured the monolayers with a polarimeter, to study the depolarization of the light produce by each monolayer. The measurement of the depolarization of the different porous silicon monolayers has been realized with a polarimeter Jobin Yvon MM-16 at the Ecole polytechnique (Palaiseau).

In Fig. 6.15 we can observe the measured depolarization of three different porosity monolayers, where P is the degree of polarization. When $P=1$ indicates that the beam is completely polarized [235]. These layers have been obtained with $J=10$ mA/cm², $J=20$ mA/cm², and $J=50$ mA/cm² and the χ^2 of the corresponding models are $\chi^2_{10} < \chi^2_{20} < \chi^2_{50}$.

The layer obtained with $J=10$ mA/cm² is the one with the lower depolarization, that is the one with P closest to the unity for the whole wavelength range. The layer obtained with $J=20$ mA/cm² presents more depolarization than the previous one. The porosity of this layer is higher than the previous layer, which could be the reason for the increment of the depolarization. The increment of depolarization indicates that this layer is more difficult to characterize with ellipsometry than the previous one, explaining the reason for $\chi^2_{10} < \chi^2_{20}$.

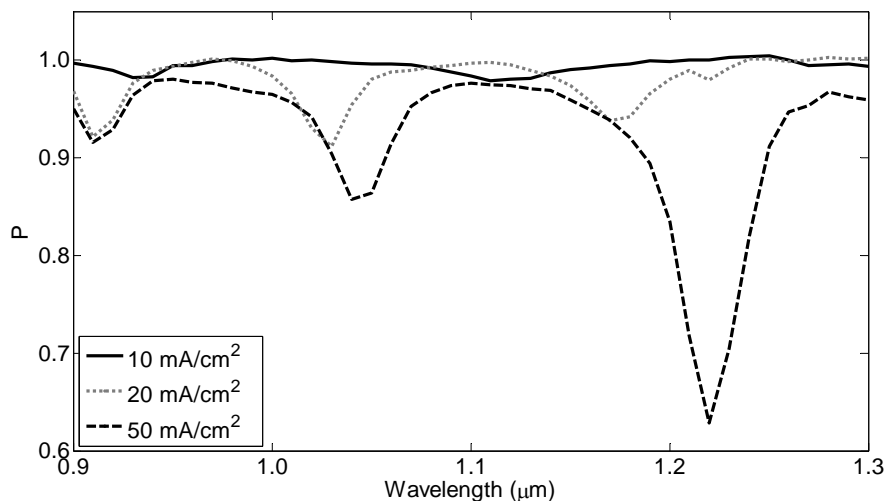


Fig. 6.15. Depolarization of three porous silicon layers with obtained with different current densities, therefore with different porosity.

The last layer analyzed is the one obtained with $J=50 \text{ mA/cm}^2$. In Fig. 6.15 we can observe that this is the layer with the highest depolarization, which explains that the ellipsometric data simulated for this layer has a higher χ^2 than the others.

We can conclude that when the current density increases, that is when the porosity increases, the depolarization of the fabricated porous silicon layer increases making more difficult the characterization of the layer using ellipsometry.

6.3.4. Summary

The results obtained with the ellipsometric characterization of the porous silicon monolayers have been summed up in Table 6.II. In this table the thicknesses obtained for the different monolayers are indicated together with the values of porosity obtained for $\lambda=1.8 \text{ }\mu\text{m}$ and the refractive indices calculated for the different optical models.

J (mA/cm ²)	Optical model	Thickness (μm)	Porosity p (%)	Refractive index n
10	Gradient	1.36	$p_{\text{top}} = 56.9$ $p_{\text{bottom}} = 46.1$	$n_{\text{top}} = 1.93$ $n_{\text{bottom}} = 2.25$
14	Gradient	1.30	$p_{\text{top}} = 60.3$ $p_{\text{bottom}} = 48.8$	$n_{\text{top}} = 1.88$ $n_{\text{bottom}} = 2.17$
20	Anisotropic	2.44	$p_{\text{ext}} = 54.3$ $p_{\text{ord}} = 60.7$	$n_{\text{ext}} = 2.01$ $n_{\text{ord}} = 1.82$
30	Anisotropic	3.28	$p_{\text{ext}} = 61.5$ $p_{\text{ord}} = 67.0$	$n_{\text{ext}} = 1.80$ $n_{\text{ord}} = 1.64$
50	Anisotropic	2.28	$p_{\text{ext}} = 70.7$ $p_{\text{ord}} = 76.3$	$n_{\text{ext}} = 1.54$ $n_{\text{ord}} = 1.40$

Table 6.I. Summary of the ellipsometric characterization of the porous silicon layers obtained with different current densities. The porosities (and its corresponding refractive index) are the values at the top and at the bottom for the isotropic gradient model and the extraordinary and ordinary values for the anisotropic optical model. The porosity and refractive index values are the ones for $\lambda=1.8 \mu\text{m}$.

In Table 6.II the refractive index and the thickness obtained with this ellipsometric characterization are compared with the ones obtained with other methods (MIF method and SEM). To ease this comparison, the averaged value of the ellipsometric refractive index is used. We can observe that the results obtained with these different methods completely agree, therefore the spectroscopic ellipsometry can be considered an appropriate method for the characterization of porous silicon layers.

J (mA/cm ²)	Optical model	$n_{\text{ellipsometry}}$ (averaged at $\lambda=1.8 \mu\text{m}$)	n_{MIF} (for λ near $1.8 \mu\text{m}$)	$d_{\text{ellipsometry}}$ (μm)	d_{SEM} (μm)	χ^2
10	Gradient	2.09	2.05	1.36	1.32	25.9
14	Gradient	1.99	1.97	1.30	1.35	81.4
20	Anisotropic	1.91	1.92	2.44	2.48	46.4
30	Anisotropic	1.72	1.73	3.28	3.28	60.5
50	Anisotropic	1.47	1.45	2.28	2.37	100.5

Table 6.II. Summary of the ellipsometric characterization of porous silicon monolayers obtained with different current densities. The results obtained with the MIF method and SEM are also presented for comparison.

In this table, it can be also observed that when the current density increases the porosity increases and therefore the refractive index decreases. The optical model used for the simulation of the ellipsometric data is different depending on the porosity of the layers: an isotropic gradient model is the appropriate for low porosity layers ($J \leq 14 \text{ mA/cm}^2$) and an anisotropic one for the high porosity layers ($J > 14 \text{ mA/cm}^2$).

6.4. Characterization of porous silicon multilayers

In this section, the ellipsometric study of porous silicon multilayers is presented. All these multilayers consist of the periodic repetition of two different porous layers: one layer was obtained with $J=20 \text{ mA/cm}^2$ and the other with $J= 50 \text{ mA/cm}^2$. The former is the lowest current density that produces an anisotropic layer whereas the latter is the highest current density used for the formation of porous silicon layers.

The anisotropic optical models obtained with the study of monolayers (section 6.3.2) are used now as a starting point for the characterization of the different layers of the multilayers.

6.4.1. One period multilayer

This multilayer consists of one period (two layers) where the top layer has been obtained with the application of $J=20$ mA/cm² for 30 s and the bottom layer with $J=50$ mA/cm² for 30 s as well. The SEM image of this multilayer is shown in Fig. 6.16, where we can observe that the bottom layer is thicker than the top layer.

The optical models obtained in the previous section for $J=20$ mA/cm² and $J=50$ mA/cm² were anisotropic. Hence, for the optical model of this multilayer we have used two anisotropic layers.

The parameters that have been determined in this model are the thickness and the porosity (ordinary and extraordinary indices) of the two layers of the stack. The resulting best fitted values of the parameters are presented in Fig. 6.17a whereas Fig. 6.17b shows the agreement between the measured and the simulated ellipsometric data, with $\chi^2=23.6$.

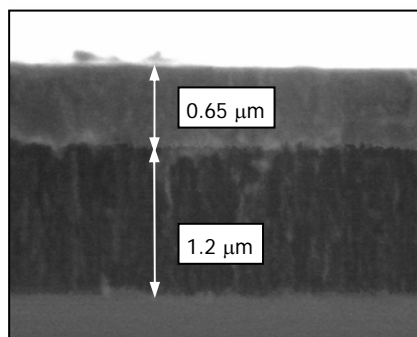


Fig. 6.16. SEM image of the one-period multilayer. Although the interface between the two porous layer is difficult to determine, the estimated thickness of the layers are approximately $d_1 \approx 0.65$ μm and $d_2 \approx 1.2$ μm .

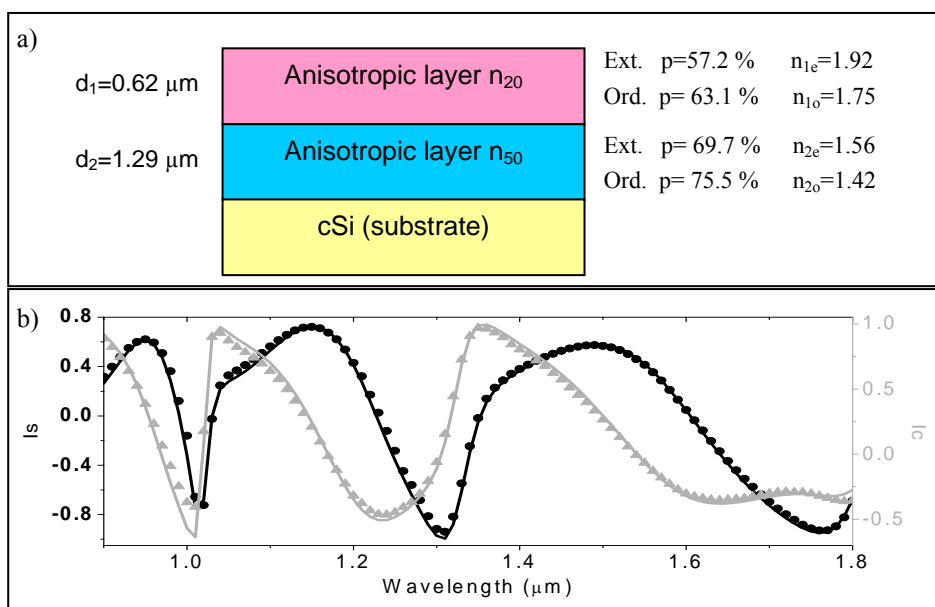


Fig. 6.17. a) Optical model consisting of two anisotropic layers and the resulting best fitted values for the corresponding parameters: thickness, porosity and refractive index ($\lambda=1.8 \mu\text{m}$) for the extraordinary and the ordinary axes b) Measured ellipsometric data (dots) and simulated ellipsometric data obtained with the optical model (line) of Fig. 6.17a.

In Fig. 6.17a, we can observe that the thicknesses d_1 and d_2 obtained with ellipsometry completely agree with the thicknesses estimated with the SEM image.

The best fitted refractive indices of these two layers are very close to the ones determined during the characterization of the corresponding monolayers, being in both cases the extraordinary refractive index higher than the ordinary. The small difference between the monolayer and the multilayer refractive indices was expected because bibliography about porous silicon suggests that the layers that form a multilayer may have a slightly different refractive index to the monolayers fabricated with the same current density [19].

6.4.2. Two period multilayer

This multilayer is formed by two periods. Each period consists of two layers. The top layer of the period has been obtained with the application of $J=20 \text{ mA/cm}^2$ for 20 s and the bottom layer with $J=50 \text{ mA/cm}^2$ for also 20 s. The SEM image of this multilayer can be observed in Fig. 6.18, where the thickness of each layer has been estimated.

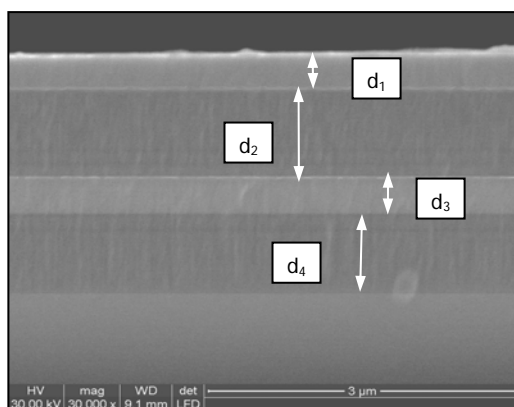


Fig. 6.18. SEM image of the two-period multilayer. Although the interface between the porous layers is difficult to determine, the estimated thickness of the layers are approximately $d_1 \approx 402 \text{ nm}$, $d_2 \approx 806 \text{ nm}$, $d_3 \approx 408 \text{ nm}$, and $d_4 \approx 826 \text{ nm}$.

The optical model used for this multilayer can be observed in Fig. 6.19a. The best fitted parameters obtained for the anisotropic monolayer model has been used as starting point for the characterization of each layer of the two period stack. In this case, the number of parameters to be fitted increased significantly: four different thicknesses and eight different porosities.

The best fitted thicknesses obtained with ellipsometry agree with the ones obtained with the SEM image, the difference between them is very small and it can be caused by the inaccuracy of the SEM image as the interface between the different layers cannot be defined clearly.

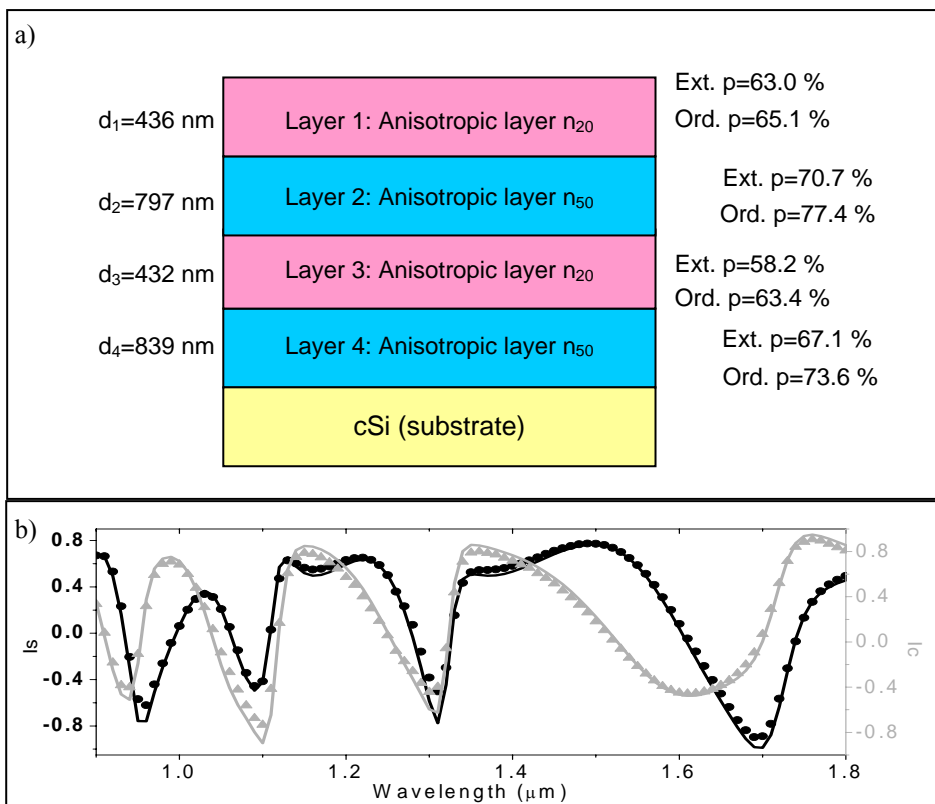


Fig. 6.19. a) Schematic representation of the ideal structure used to build the optical model consisting of four anisotropic layers (two periods) together with the best fitted values of the variable parameters: thickness and porosity for the extraordinary and the ordinary indices b) Measured (dots) and simulated (solid line) ellipsometric data obtained with the optical model shown in Fig. 6.19a. .

Concerning the porosities (refractive indices), we can observe that for both current densities the porosities are very close to the respective monolayers but they slightly decrease with depth. We can observe that the porosity of layer 1 is slightly higher than the porosity of layer 3 although they have been fabricated with the same current density. The same happens with layers 2 and 4. This variation in depth can be explained by the chemical etching that acts on the outer layers and that adds its contribution to that of the initial electrochemical

etching. Hence, it is usual for the outer layers to have a higher porosity than the inner layers obtained with the same current densities. The ellipsometric results corroborate this fact.

Fig. 6.19b compares the measured ellipsometric data with the ones obtained with the simulation of the optical model shown in Fig. 6.19b. The difference is very low, $\chi^2=48.9$, considering the high number of parameters to be determined in the optical model.

6.4.3. Three period multilayer

This multilayer is formed by three periods (six layers). The top layer of the period has been obtained with the application of $J=20$ mA/cm² for 20 s and the bottom layer with $J=50$ mA/cm² for also 20 s. The SEM image of this multilayer can be observed in Fig. 6.20, where the thickness of each layer has been estimated. These thickness values are approximate because the SEM image does not allow an exact measurement due to the roughness of the interfaces, so we can consider that the error introduced in these estimations can be around 10-15 %.

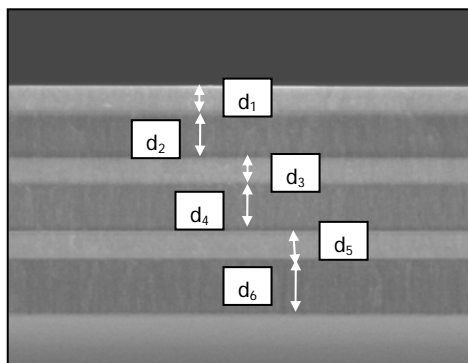


Fig. 6.20. SEM image of the three-period multilayer. The interfaces between the different porous layers can be seen. The thickness of the layers are approximately $d_1 \approx 440$ nm, $d_2 \approx 790$ nm, $d_3 \approx 370$ nm, $d_4 \approx 775$ nm, $d_5 \approx 411$ nm, and $d_6 \approx 848$ nm.

Fig. 6.21a shows the optical model realized for this multilayer where the variable parameters to be fitted are the thicknesses and the porosities (ordinary and extraordinary) of all the layers.

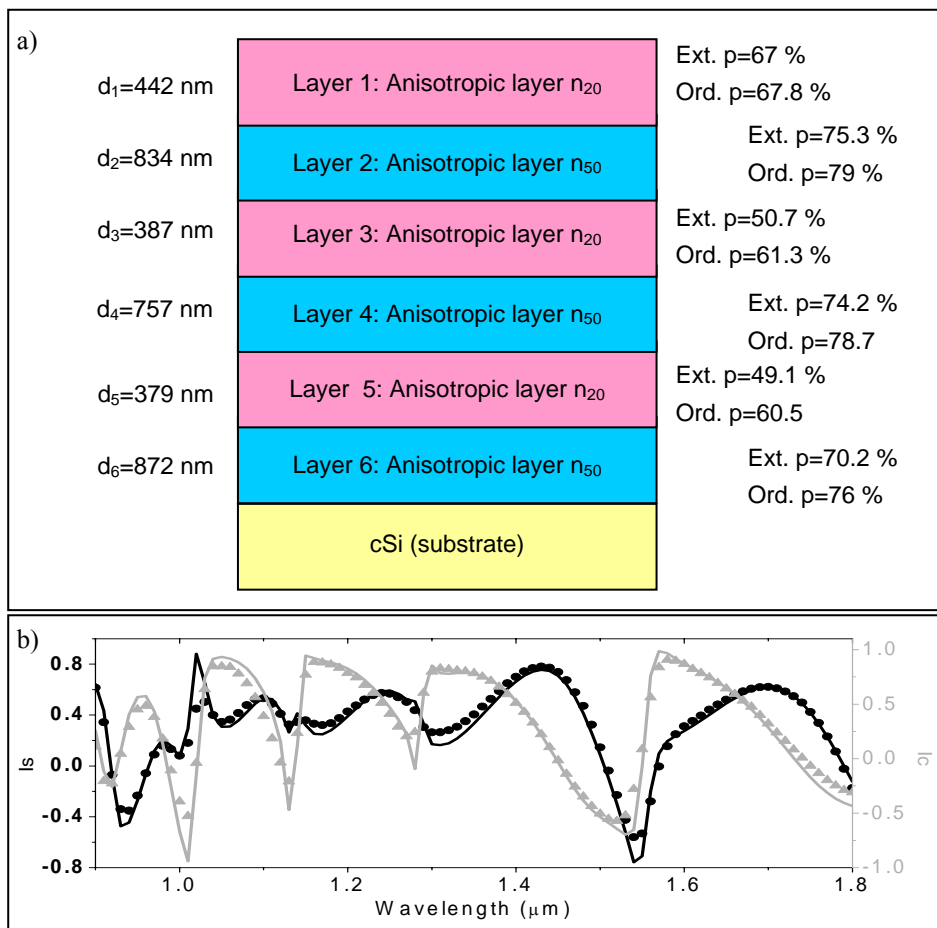


Fig. 6.21. a) Schematic representation of the ideal structure used to build the optical model consisting of six anisotropic layers (three periods) together with the best fitted values of the variable parameters: thickness and porosity for the extraordinary and the ordinary indices. b) Measured (dots) and simulated (solid line) ellipsometric data obtained with the optical model shown in Fig. 6.21a.

The number of parameters to be determined is very high, concretely 18, which increases the difficulty of finding an accurate fit. Many different values of these parameters give a good agreement between the simulated and the measured ellipsometric data. But not all of these fits are correct because their physical meaning can be contradictory with the characteristics of the multilayer that are *a priori* known, i.e. layer thicknesses or porosities very different to the expected. Here we present one of the best fits obtained that provided parameters that are in accordance with the expected values.

If we start considering the porosities of the layers we can observe that layers obtained with the same current density have different values of their respective porosity that depends on the depth. We have observed that the porosity decreases with depth. This effect has also been observed for stacks of two periods and a discussion is provided above in the text and in the bibliography. This porosity variation with depth happens for both types of layers, 20 mA/cm² and 50 mA/cm². We can also see that the porosities of these layers are similar to the ones obtained with the analysis of the respective monolayers but there is a difference between them that is higher when the thickness of the multilayer increases.

The differences between the measured and the simulated ellipsometric data can be observed in Fig. 6.21b, where $\chi^2=156.3$. This error is higher than the ones of the previous multilayers. This is due to the higher number of layers of the multilayer to be characterized.

6.5. Conclusions

The ellipsometric characterization of porous silicon monolayers and multilayers has been realized. This characterization has determined the main physical characteristics of these layers, porosity (and therefore refractive index) and thickness; and has permitted the analysis of their anisotropy.

The refractive index of the porous material was modeled with the Bruggeman effective medium approximation (EMA) by assuming a mixture of crystalline silicon and void. For low porosities, the optical behavior of the

samples has been modeled with a graded index model. However, as porosity of the monolayers increases, the gradient index model is no longer valid, and it must be substituted by another one consisting of an anisotropic uniaxial layer with its optical axis oriented perpendicular to the surface of the sample. From the ellipsometric study, we demonstrate that the anisotropy increases with the porosity. The depolarization of light caused by sample thickness non-uniformity has been measured and used to estimate the quality of measurements as well as the adequacy and goodness of ellipsometric data fits. These monolayers have been also analyzed by spectroscopic reflectometry, using a FTIR spectrometer, and by scanning electron microscopy (SEM). A good agreement has been observed between the refractive indices and thicknesses obtained with these methods and the values estimated with the spectroscopic ellipsometry.

Apart from the monolayers, we have also studied multilayers consisting of a periodic repetition of two layers with different degrees of porosity. The thicknesses of the layers that form the multilayers have been determined by ellipsometry and they agree with the values obtained with the SEM analysis. The porosity of these layers have been also studied, a characteristic of the multilayers that could not be to analyze with any of the other characterization methods used. We have observed that the anisotropic models obtained from the study of the monolayers can be used as a starting point for the characterization of the different layers of the multilayers. However, the ellipsometric measurements revealed that there is a slight difference between the layers appertaining to the multilayer, and the corresponding monolayers obtained with identical fabrication parameters. In a multilayer, the layers fabricated with the same current density do not have the same porosity but it decreases with depth. This means that there is a gradient of porosity with depth.